Received: 26 January 2024 | Revised: 10 June 2024 | Accepted: 11 June 2024

DOI: 10.1111/jnc.16158

Journal of Neurochemistry JNC The Official Journal of the International Society for Neurochemistry WILEY

ORIGINAL ARTICLE

Glyceraldehyde metabolism in mouse brain and the entry of blood-borne glyceraldehyde into the brain

Bjørnar Hassel[1,2,3] | Kristian Sørnes[4] | Ahmed Elsais[5] | Patricia Reyes Cordero[4] | Anne Sofie Frøland[1,4] | Frode Rise[4]

[1]Department of Neurohabilitation, Oslo University Hospital, Oslo, Norway

[2]Norwegian Defence Research Establishment (FFI), Kjeller, Norway

[3]Institute of Clinical Medicine, University of Oslo, Oslo, Norway

[4]Department of Chemistry, University of Oslo, Norway

[5]Department of Neurology, Oslo University Hospital, Oslo, Norway

Correspondence
Bjørnar Hassel, Department of Complex Neurology and Neurohabilitation, Oslo University Hospital, Kirkevn 166, 0450 Oslo, Norway.
Email: bjornar.hassel@medisin.uio.no

Abstract

D-Glyceraldehyde, a reactive aldehyde metabolite of fructose and glucose, is neurotoxic in vitro by forming advanced glycation end products (AGEs) with neuronal proteins. In Alzheimer's disease brains, glyceraldehyde-containing AGEs have been detected intracellularly and in extracellular plaques. However, little information exists on how the brain handles D-glyceraldehyde metabolically or if glyceraldehyde crosses the blood–brain barrier from the circulation into the brain. We injected [U-^{13}C]-D-glyceraldehyde intravenously into awake mice and analyzed extracts of serum and brain by ^{13}C nuclear magnetic resonance spectroscopy. ^{13}C-Labeling of brain lactate and glutamate indicated passage of D-glyceraldehyde from blood to brain and glycolytic and oxidative D-glyceraldehyde metabolism in brain cells. ^{13}C-Labeling of serum glucose and lactate through hepatic metabolism of [U-^{13}C]-D-glyceraldehyde could not explain the formation of ^{13}C-labeled lactate and glutamate in the brain. Cerebral glyceraldehyde dehydrogenase and reductase activities, leading to the formation of D-glycerate and glycerol, respectively, were 0.27–0.28 nmol/mg/min; triokinase, which phosphorylates D-glyceraldehyde to D-glyceraldehyde-3-phosphate, has been demonstrated previously at low levels. Thus, D-glyceraldehyde metabolism toward glycolysis could proceed both through D-glycerate, glycerol, and D-glyceraldehyde-3-phosphate. The aldehyde group of D-glyceraldehyde was overwhelmingly hydrated into a diol in aqueous solution, but the diol dehydration rate greatly exceeded glyceraldehyde metabolism and did not restrict it. We conclude that (1) D-glyceraldehyde crosses the blood–brain barrier, and so blood-borne glyceraldehyde could contribute to AGE formation in the brain, (2) glyceraldehyde is taken up and metabolized by brain cells. Metabolism thus constitutes a detoxification mechanism for this reactive aldehyde, a mechanism that may be compromised in disease states.

KEYWORDS
advanced glycation end product, Alzheimer's disease, blood–brain barrier, diabetes, diol dehydration, glyceraldehyde

Abbreviations: AGE, advanced glycation end products; GABA, γ-aminobutyric acid; i.v., intravenous; NMRS, nuclear magnetic resonance spectroscopy; TCA cycle, tricarboxylic acid cycle; TMSP, trimethylsilylpropionate.

1 | INTRODUCTION

D-Glyceraldehyde (hereafter "glyceraldehyde") is a reactive metabolite of several precursors, among them glucose, fructose, glycerol, and glycerate (Hassel et al., 2015; Hoffman et al., 1980; Leicht et al., 1978; O'Brien & Schofield, 1980; Stewart et al., 1967). Glyceraldehyde may react with proteins, leading to the formation of advanced glycation end products (AGEs). In vitro, glyceraldehyde has been shown to form neurotoxic AGEs with β-tubulin (Ooi et al., 2022). Immunopathological studies of brains of Alzheimer's disease patients have suggested the presence of intracellular glyceraldehyde-containing AGEs in neurons in the hippocampus and parahippocampal gyrus (Choei et al., 2004), whereas other studies have suggested that glyceraldehyde forms AGEs with extracellular beta-amyloid-containing plaques (Fawver et al., 2012; Piccirillo et al., 2023).

Glyceraldehyde is a hydrophilic, non-ionic molecule with a low estimated octanol:water partition coefficient of 0.02 (logP = −1.7) and a predicted solubility in water of 9 mol/L (The Human Metabolome Database, n.d.). Therefore, glyceraldehyde would be expected to cross the phospholipid bilayer of plasma membranes by means of a transporter or a channel. A non-saturable transport mechanism for glyceraldehyde was partly characterized in insulinoma cells (Davies et al., 1994), but the extent to which glyceraldehyde would be transported into brain cells is unknown, although uptake of radiolabeled glyceraldehyde at low concentration has been reported (Hassel et al., 2015). Also unknown is whether blood-borne glyceraldehyde, can cross the blood–brain barrier, contributing to AGE and beta-amyloid plaque formation in the brain. Glyceraldehyde has been detected at micromolar concentration in blood, and blood levels are increased in diabetes (Martin-Morales et al., 2021). The association between diabetes and Alzheimer's disease (Biessels & Despa, 2018) adds clinical interest to the question of glyceraldehyde movement across the blood–brain barrier, as does the finding that blood–brain barrier dysfunction, allowing plasma factors into the brain parenchyma, may be an early feature of Alzheimer's disease (Montagne et al., 2020).

Glyceraldehyde could enter several metabolic pathways. It could become phosphorylated by triokinase to glyceraldehyde-3-phosphate, which may enter the glycolytic pathway or disintegrate into methylglyoxal and phosphate (Phillips & Thornalley, 1993). Methylglyoxal is prone to metabolism along the glyoxalase pathway, leading to the formation of metabolically inert D-lactate. Alternatively, glyceraldehyde could become reduced to glycerol or oxidized to D-glycerate, both of which may become phosphorylated (by glycerol kinase and glycerate kinase, respectively) and eventually enter the glycolytic pathway, leading to the formation of pyruvate and, possibly, L-lactate. The kinases that phosphorylate glyceraldehyde, glycerol and glycerate are all expressed in rodent brain, although at low levels (Hassel et al., 2015; Jenkins & Hajra, 1976).

In aqueous solution, the aldehyde group of glyceraldehyde becomes hydrated to a diol (Figure 1; Angyal & Wheen, 1980; Serianni et al., 1979). The rate of (spontaneous) dehydration of an aldehyde group to its free aldehyde may affect aldehyde metabolism (Guengerich et al., 2011). Whether dehydration of the glyceraldehyde diol would impede glyceraldehyde metabolism in the brain is not known.

In order to investigate the metabolism of glyceraldehyde in the brain in vivo, including whether or not glyceraldehyde crosses the blood–brain barrier, we injected ^{13}C-labeled glyceraldehyde intravenously (i.v.) into mice and analyzed serum and organ extracts by ^{13}C nuclear magnetic resonance spectroscopy (NMRS). Further, we calculated the rate of dehydration of hydrated glyceraldehyde to a free aldehyde, which we assume to be the metabolizable form. Lastly, we measured the activity of glyceraldehyde-reducing and glyceraldehyde-oxidizing enzymes and the activity of glyoxalase I and II in the brain.

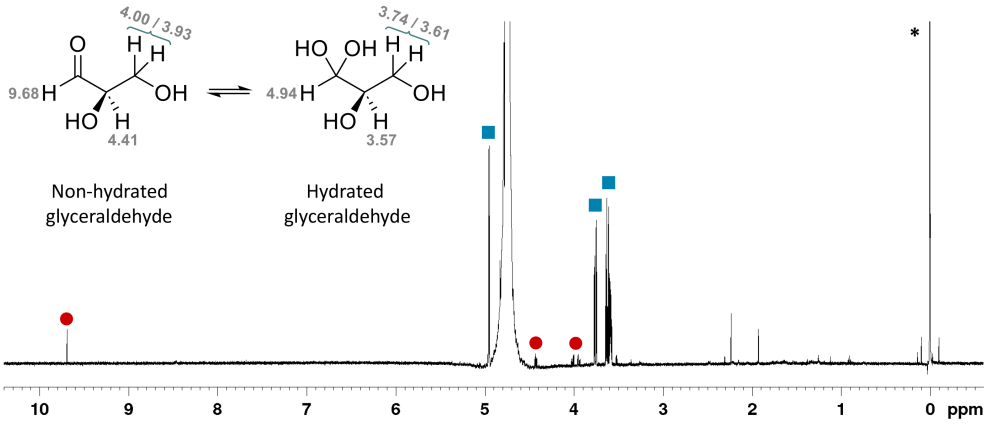

FIGURE 1 ^{1}HNMR spectrum (600 MHz) of non-labeled D-glyceraldehyde, 3.0 mmol/L, in D_2O at 25°C. Signals from non-hydrated glyceraldehyde are marked with red circles; signals from hydrated glyceraldehyde are marked with blue squares. Chemical shift values are given relative to TMSP at 0.0 ppm (*). Top left: Structure of non-hydrated and hydrated glyceraldehyde, with chemical shifts assigned. Signals at 4.94 and 9.68 ppm correspond to the hydrated and non-hydrated aldehyde groups, respectively. The large peak at 4.8 ppm represents water.

2 | MATERIALS AND METHODS

The animals were outbred female NMRI mice (model no. NMRI-F; Bomholt, Ry, DK). They were 10 weeks old at arrival at our research institute and were used after 7 days of acclimatization (11 weeks old); they then weighed approximately 30 g. The animals were caged in groups of five in plastic cages with a floor space of 26.5 × 42 cm^2 and a height of 15.5 cm. Animals had free access to food and tap water; air humidity was 50%, room temperature was 22°C, and the light/dark cycle was 12 h (7 a.m./7 p.m.). Animal treatment adhered to national ethical guidelines and the EU Directive 2010/63/EU for animal experiments (European Union, 2010), and experiments were ethically approved by national authorities (Forsøksdyrutvalget, approval# FDU2142/2009). All efforts were made to minimize animal suffering and to reduce the number of animals used.

In total, 37 mice were used (eight cages). Twenty-seven animals were used for in vivo isotopic labeling studies with [U-^{13}C]glyceraldehyde; 10 animals were used for enzymatic studies (Figure S1). Sample sizes were determined from previous studies (Gonzalez et al., 2005; Hassel et al., 2015; Hassel & Bråthe, 2000; Nguyen et al., 2003) and were based on the purpose of investigating whether glyceraldehyde may cross the blood–brain barrier from the circulation into the brain. Sample sizes were a compromise between the need to assess data reproducibility and the need to limit the number of animals used. No exclusion criteria were predetermined, and no animal was excluded from the analyses. Randomization was not included. Groups were only compared with respect to the effect of insulin treatment, and a group of animals that did not receive insulin served as control. We used female mice as we have done in previous studies (Gonzalez et al., 2005; Hassel et al., 2015; Hassel & Bråthe, 2000; Nguyen et al., 2003). An earlier study did not find any difference in the metabolism of ^{13}C-labeled pyruvate, which with respect to its metabolism is closely related to glyceraldehyde, in female and male mice (Gonzalez et al., 2005).

[U-^{13}C]- D-glyceraldehyde, 98% ^{13}C enrichment, 100 mmol/L water, was from Omicron (South Bend, IN, USA; catalog number GLE-006). Prior to experiments, sodium chloride was added at 100 mmol/L to achieve physiologic osmolarity. pH was adjusted to 7. Other reagents were from Sigma-Aldrich (St. Louis, MO, USA). Insulin 100 U/mL was from Sanofi (Sanofi Winthrop Industrie, France).

2.1 | In vivo ^{13}C-labeling from [U-^{13}C] glyceraldehyde

Animal experiments took place between 8 and 10 a.m. Twenty-seven mice were used for ^{13}C-labeling experiments (Figure S1). Prior to experiments, mice were fasted for 12 h with free access to drinking water. This was done to reduce serum glucose concentration, because fed animals have reduced label incorporation into brain metabolites, as has been documented earlier in studies on the cerebral metabolism of ^{13}C-labeled lactate and pyruvate given i.v. (Gonzalez et al., 2005; Hassel & Bråthe, 2000). Eight out of the 27 mice were pretreated with subcutaneous (s.c.) insulin, 3 U/g bodyweight. This was done to further reduce the serum concentration of glucose.

All animals received an i.v. bolus injection of [U-^{13}C]glyceraldehyde, 100 mmol/L (containing NaCl, 100 mmol/L), 10 μL/g bodyweight, over 10 s into a tail vein (corresponding to 1 μmol [U-^{13}C] glyceraldehyde/g bodyweight) through a 30G cannula. The injected fluid was at room temperature, approximately 22°C. After i.v. and s.c. injections, animals were returned to their home cage. The animal procedures may seem to be at the severe end of what is allowed in the EU; however, the injection volume and injection rate were well within values in university guidelines on animal handling (e.g., Indiana University, 2022; University of British Columbia, 2021).

After injection of [U-^{13}C]glyceraldehyde, three mice were killed at 15 s, four were killed at 1, 5, 10, and 15 min after completion of the injection of [U-^{13}C]glyceraldehyde. The eight animals that had been pretreated with insulin received [U-^{13}C]glyceraldehyde i.v. at 90 min after injection of insulin. Four out of these mice were killed at 10 min, four at 15 min after the injection of [U-^{13}C]glyceraldehyde.

The animals were killed by cervical dislocation and decapitation in a room separated from the littermates. The heads were immediately frozen in liquid nitrogen. Blood was collected from the severed neck vessels, and livers, lungs, hearts, and spleens were rapidly dissected out and frozen in liquid nitrogen.

Whole brains (including cerebellum and brain stem), livers, lungs, hearts, and spleens were weighed in the frozen state before being homogenized 1:10 (weight/volume) in 7% perchloric acid (vol/vol). Blood was centrifuged, and serum was mixed 1:1 with 7% perchloric acid (this did not apply to samples from animals that were sacrificed 15 s after injection of [U-^{13}C]glyceraldehyde (see below)). Protein was removed by centrifugation, and supernatants were neutralized with KOH, 9 mol/L. The water phase was lyophilized to dryness and redissolved in 500 μL D_2O containing 0.1% dioxane as an internal concentration standard. Serum from a group of mice with 15 s survival after injection of [U-^{13}C]glyceraldehyde was not treated with perchloric acid but was analyzed without prior removal of proteins; this was done to avoid any possible alteration to [U-^{13}C]glyceraldehyde by perchloric acid or KOH.

2.2 | Nuclear magnetic resonance spectroscopy

^{1}H NMRS was performed on a Bruker Avance I 600 MHz spectrometer equipped with a TCI cryoprobe and an automatic sample changer. Of each sample 32 scans were collected into 64 k data points, using the Bruker "noesygppr1d" sequence with a spectral width of 20.6 ppm, 2.65 s acquisition time, and a 4.0 s relaxation delay. An exponential line broadening of 0.3 Hz was applied, and the Fourier-transformed spectra were referenced relative to trimethylsilylpropionate-d_4 sodium salt (TMSP, δ = 0.00 ppm). TMSP was added to the samples at a final concentration of 2.9 mmol/L. The temperature of the samples was kept at 25°C, except when determining the concentration of non-hydrated, monomeric glyceraldehyde at 37°C, as described in Section 3.

^{13}CNMRS was performed with a 30° pulse angle and 39.6 kHz spectral width with 64 k data points, an acquisition time of 0.8258 s, and a 3 s relaxation time; 5120 scans were obtained per sample (Hassel & Bråthe, 2000). The spectra were referenced relative to dioxane (δ = 67.0 ppm), which was added as an internal concentration standard. The amount of ^{13}C-labeled lactate, glutamate, or glucose relative to dioxane was then calculated from the spectra. The percent ^{13}C enrichment of metabolites in brain, liver, and serum was calculated from doublets that represented labeling of lactate C_3, glutamate C_4, GABA C_2, or glucose C_1 from [U-^{13}C]glyceraldehyde divided by the total amount of lactate, glutamate, or glucose, which was calculated from the singlets that represented naturally abundant ^{13}C in lactate C_3, glutamate C_4, or glucose C_1; naturally abundant ^{13}C is 1.1% of total carbon (see, for example, Gonzalez et al., 2005, for typical ^{13}CNMRS spectra of lactate C_3, glutamate C_4, and GABA C_2). In this way, we measured naturally abundant and label-derived ^{13}C by the same method in the same sample. Lactate that is ^{13}C-labeled in the C_3 position from [U-^{13}C]glyceraldehyde will also have a ^{13}C in the neighboring C_2 position as well as in the carboxyl C_1 position. Similarly, glutamate that is ^{13}C-labeled in the C_4 position will also have a ^{13}C in the carboxyl C_5 position, and glucose labeled in the C_1 position will have a ^{13}C in the C_2 position. These neighboring ^{13}C carbons will cause the signals from lactate C_3, glutamate C_4, and glucose C_1 to split into doublets, but they will have virtually no effect on the relaxation of these carbons compared to the surrounding protons. This is because relaxation due to neighboring nuclei scales with the gyromagnetic ratio squared and inversely with the bond length to the sixth power (Keeler, 2010). Since ^{13}C has a gyromagnetic ratio of around 1/4 that of 1H, and the C3–C2 bond of, for example, lactate is around 40% longer than the nearby C-H bonds (Zhang et al., 2019), this equates to less than 1% of the relaxation effect of surrounding protons. Therefore, calculating the percent ^{13}C enrichment of lactate, glutamate, and glucose from doublets and singlets in the same ^{13}CNMRS spectra will yield true percent enrichment values. The integration of the ^{13}C NMRS was done blindly with respect to the treatment of the animals.

2.3 | Calculation of glyceraldehyde dehydration

Glyceraldehyde dehydration rate constants were derived from ^{1}H selective inversion recovery experiments acquired on Bruker Avance I and Avance II 600 MHz NMR spectrometers, equipped with a TCI cryoprobe and a TXI room temperature probe, respectively. Experiments were performed using an in-house made "selt1ir" pulse sequence (Supporting information S1), consisting of an initial selective 180° pulse, a mixing time, a non-selective 90° pulse followed by acquisition. Before acquiring spectra, the hydrated aldehyde signal of hydrated glyceraldehyde (4.94 ppm) was selected for inversion by the 180° pulse.

Repeated acquisitions with varying mixing times produced pseudo-2D datasets that were processed as T_1 relaxation data in Bruker's TopSpin 3.5 software, with signal area as the parameter of interest. Both the hydrated aldehyde signal (4.94 ppm) and the aldehyde signal of monomeric, non-hydrated glyceraldehyde (9.68 ppm) were processed in this way.

The resulting recovery data were given as input to the selective inversion recovery data fitting program CIFIT made by Bain and Cramer (1996); see their website www.chemistry.mcmaster.ca/bain/ for downloadable files and user manual. The model was assumed to be a 2-site-1-process system, with aldehyde and hydrate representing the two sites and hydration/dehydration being the only dynamic process. Given the dilute concentrations in this study, any change in signal area of HDO in D_2O was assumed to be negligible and was therefore left out of the model.

With these assumptions, CIFIT uses seven parameters to model the recovery data and performs an iterative fitting of the model to the raw data until convergence is achieved. Initial values for all variables are provided by the user in advance. The parameter values that represent the best fit are then given as output by the program. One of these parameters is the dehydration rate constant, which is the variable of interest in this study. CIFIT allows any number of the seven parameters to be constrained to their initial value, meaning they are kept constant during the fitting process.

For measurements performed at 25°C, an unbiased use of CIFIT did not provide a satisfying fit between model and data. Better fits could be achieved by constraining the dehydration rate constant, as well as the T_1 relaxation rate and the magnetizations of the non-hydrated aldehyde signal, to specific values. The Python script "CIFITSCAN" was made in-house to determine these constraints in a systematic way (Supporting information S2). Through the script, CIFIT is repeatedly executed with a particular parameter of interest constrained, but with slight changes to its initial value between each run. The goodness-of-fit (root mean square deviation) for each run is recorded as a function of the scanned parameter. Best-fit values for T_1 relaxation rates as well as the dehydration rate constant were determined in this manner. Error estimations for the resulting dehydration rate constants are given as 95% confidence intervals by linear *F*-test, as described by Bain and Cramer (1996).

All ^{1}H selective inversion recovery experiments were acquired with a 20.0 ppm spectral window and Fourier-transformed with an exponential line broadening of 0.3 Hz applied to the free induction decay.

With a 300 mmol/L sample of glyceraldehyde in unbuffered, neutral D_2O, an experiment was acquired at 25°C through eight scans collected into 168 266 data points with an acquisition time of 7.0 s per scan. The relaxation delay between scans was 50.0 s, and the mixing times spanned 50 non-uniform values from 0.025 to 60.0 s. With a 30 mmol/L sample in D_2O, an experiment was acquired at 25°C through 12 scans collected into 168 266 data points with an acquisition time of 7.0 s per scan. The relaxation delay between scans was 50.0 s, and the mixing times spanned 48 non-uniform values from 0.025 to 50.0 s.

A sample of glyceraldehyde at 100 mmol/L in unbuffered, neutral D_2O at 37°C, underwent 12 scans collected into 72 114 data points, with an acquisition time of 3.0 s per scan. The relaxation

delay between scans was 62.0 s, and the mixing times spanned 52 non-uniform values from 0.025 to 70.0 s.

2.4 | Metabolite and enzyme analyses

Separation and quantitation of amino acids were done by high-performance liquid chromatography and fluorescence detection after pre-column derivatization with *o*-phthaldialdehyde (Dahlberg et al., 2014). Serum concentrations of glucose and lactate were measured by reflectance spectrophotometry with an Ektachem DT60 (Kodak, Rochester, NY, U.S.A).

Ten mice were used for enzyme analyses: five for aldehyde dehydrogenase and reductase activities, and five for glyoxalase activities. Enzyme analyses were done with 10% homogenates (weight/volume) of whole mouse brain or liver in sucrose, 0.32 mol/L. Prior to experiments, the homogenates were treated with Triton X-100, final concentration 0.3% (vol/vol), and centrifuged at 5000 *g*. The supernatants were used for analyses. Reactions took place at 37°C in a 100 μL quartz cuvette (Starna, Hainhault, Essex, UK), and changes in absorbance were followed in a Shimadzu UV 160 spectrophotometer. The reactions were linear with the amount of homogenate added and with time for at least 3 min.

Aldehyde dehydrogenase activity in brain and liver was measured spectrophotometrically as the formation of NADH at 340 nm (Moon et al., 2007). The reaction mixture was [U-^{13}C]glyceraldehyde, 3 mmol/L, NAD^+, 2 mmol/L, EDTA, 1 mmol/L, and Triton X-100, 0.1% (vol/vol), in sodium pyrophosphate, 60 mmol/L, pH 8.25; total volume 860 μL. The reaction was started by adding 50 μL of the supernatants from brain or liver homogenates.

Aldehyde reductase activity in brain and liver was measured spectrophotometrically as loss of NADPH at 340 nm (Bohren et al., 1991). The reaction mixture was [U-^{13}C]glyceraldehyde, 3 mmol/L, NADPH, 0.15 mmol/L, in sodium phosphate, 100 mmol/L, pH 7; total volume 850 μL. The reaction was started by adding 50 μL of the supernatants from brain or liver homogenates.

Glyoxalases I and II were analyzed as described by Arai et al. (2014). Briefly, for the glyoxalase I assay, methylglyoxal, 4 mmol/L, and reduced glutathione, 4 mmol/L, both in sodium phosphate, 100 mmol/L, pH 6.6, were mixed 1:1 and incubated for 10 min at 37°C to form a hemithioacetal. In a 100 μL quartz cuvette, 80 μL of the hemithioacetal solution were mixed with 10 μL of the supernatant of the brain homogenates. For the glyoxalase II assay, 80 μL *S*-lactoyl-glutathione, 0.375 mmol/L, in Tris–HCl buffer, 50 mmol/L, pH 7.4, were mixed with 10 μL of the supernatant of the brain homogenates. The glyoxalase I and II reactions were followed by an increase or decrease in absorbance, respectively, at 240 nm.

2.5 | Data presentation and statistics

The main outcome measurement of the ^{13}C-labeling studies is the percent ^{13}C enrichment of glutamate and lactate in the brain and of glucose and lactate in serum together with the serum concentration of [U-^{13}C]glyceraldehyde. Metabolite levels are given as nmol/mg tissue wet weight or (in serum) as mmol/L. Enzyme activities are given as nmol per mg tissue wet weight per minute. Dehydration rate constants are given with 95% confidence intervals. Group comparisons were done with Student's two-tailed *t*-tests, using Graph Pad Prism version 5.0a (Boston, MA, USA), because data were continuous, without correcting for multiple comparisons or assessing normality. *P*-values <0.05 were considered statistically significant. We did not use a test to identify outliers, and no outliers were excluded from the datasets.

3 | RESULTS

3.1 | The hydration (diol) state of glyceraldehyde in solution

^{1}HNMRS showed that glyceraldehyde (unlabeled) was overwhelmingly present as a hydrated (diol) monomer in aqueous solution in agreement with previous studies (Angyal & Wheen, 1980; Serianni et al., 1979; Figure 1). A small peak at 9.68 ppm represented the hydrogen of the non-hydrated aldehyde group. In hydrated glyceraldehyde, this hydrogen is present as a doublet at 4.94 ppm. The ratio of non-hydrated: hydrated glyceraldehyde remained constant at 1:10 at 37°C over a concentration range of 3–300 mmol/L. At 25°C (the approximate temperature of the [U-^{13}C]glyceraldehyde that was injected i.v. into the animals), the ratio of non-hydrated: hydrated glyceraldehyde was constant at 1:16.

Several smaller peaks in the spectra with glyceraldehyde at 10–300 mmol/L showed that glyceraldehyde was also present as multiple dioxane dimers (not shown)—a preferred state when glyceraldehyde is dissolved in dimethyl sulfoxide (Angyal & Wheen, 1980; García-Jiménez et al., 2005). These dioxane signals increased with increasing concentration of glyceraldehyde. Thus, the dioxane signals accounted for 19% of the total ^{1}HNMRS signal with glyceraldehyde at 300 mmol/L at 37°C and for 25% of the total signal at 25°C. With glyceraldehyde at 3 mmol/L, no dioxane signals could be seen.

^{13}CNMRS of [U-^{13}C]glyceraldehyde showed three major peaks at 62.5, 74.7, and 90.3 ppm (Figure 2), representing the three carbons of hydrated glyceraldehyde, one of which (at 90.3 ppm) is the hydrated aldehyde group (Angyal & Wheen, 1980). Non-hydrated glyceraldehyde was seen as three much smaller peaks at 61.3, 78.4, and 205.1 ppm, the peak at 205.1 ppm representing the non-hydrated aldehyde carbonyl. As seen with ^{1}HNMRS, the ratio of non-hydrated:hydrated glyceraldehyde remained constant at approximately 1:16 at 25°C with [U-^{13}C]glyceraldehyde at 1–50 mmol/L.

3.2 | Rate of glyceraldehyde dehydration

The rate constant for the dehydration of unlabeled glyceraldehyde in unbuffered, neutral D_2O at 25°C was $0.036 \pm 0.001\ s^{-1}$ at

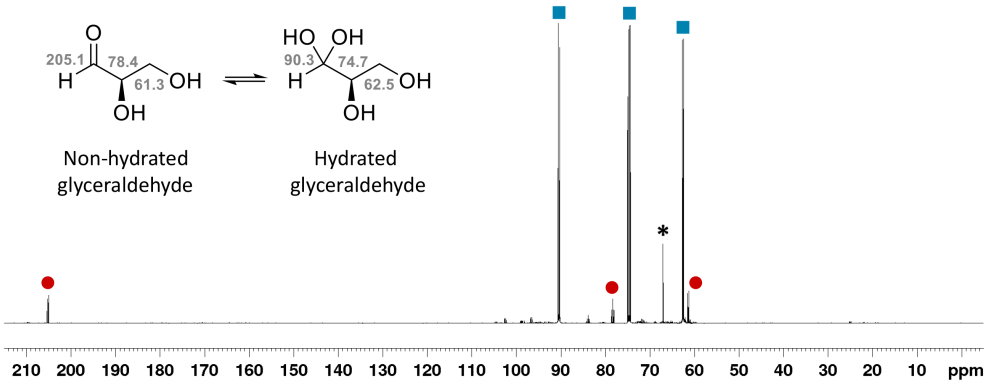

FIGURE 2 Inverse-gated ^{13}CNMR spectrum (600 MHz) of [U-^{13}C]-D-glyceraldehyde, 50 mmol/L, in D_2O at 25°C. Signals from non-hydrated glyceraldehyde are marked with red circles; signals from hydrated glyceraldehyde are marked with blue squares. Chemical shift values are given relative to 1,4dioxane at 67.0 ppm (*). Top left: Structure of non-hydrated and hydrated glyceraldehyde, with chemical shifts assigned. Signals at 90.3 and 205.1 ppm correspond to the hydrated and non-hydrated carbonyl groups, respectively.

300 mmol/L, and 0.032 ± 0.002 s^{-1} at 30 mmol/L. These values agree with a previously reported dehydration rate constant of 0.030 s^{-1} for glyceraldehyde at 25°C (Rendina et al., 1984), and they agree with the rate constant being independent of glyceraldehyde concentration at constant temperature. This is supported by the observation that the ratio between hydrated and non-hydrated glyceraldehyde is constant across a 3–300 mmol/L concentration range, which implies fixed values for the rate constants as per the law of mass action. At 37°C, the 100 mmol/L sample produced a rate constant of 0.057 ± 0.001 s^{-1}.

With an in vivo concentration of glyceraldehyde at ~1.0 nmol/mg tissue (~1 mmol/L; see next paragraph for the serum concentration of glyceraldehyde), a dehydration rate constant of 0.057 s^{-1} at 37°C corresponds to a reaction rate of 3.1 nmol/mg/min, because glyceraldehyde is 91% hydrated at this temperature (0.057 s^{-1} × 60 s/min × 0.91 × 1.0 nmol/mg tissue). Using the lowest estimated rate constant of 0.032 s^{-1} at 25°C, the rate is 1.8 nmol/mg tissue/min because glyceraldehyde is 94% hydrated at this temperature (0.032 s^{-1} × 60 s/min × 0.94 × 1.0 nmol/mg tissue). The oxidative metabolic rate for glucose in mouse brain has been estimated at ~1 nmol/mg tissue/min (Kamp et al., 1980; Xin et al., 2015). As will be seen below, [U-^{13}C]glyceraldehyde contributed only a few percent to the formation of glutamate, and so the metabolic rate for [U-^{13}C]glyceraldehyde was much lower than the overall cerebral metabolic rate of ~1 nmol/mg tissue/min, which means that the glyceraldehyde dehydration rate greatly exceeded glyceraldehyde metabolism and that dehydration of the aldehyde group did not determine the metabolic rate for glyceraldehyde.

3.3 | ^{13}C-labeled compounds in serum

Overnight fasting produced concentration of glucose in serum of 3.3 ± 0.5 mmol/L (n = 8) prior to injection of [U-^{13}C]glyceraldehyde. I.v. injection of [U-^{13}C]glyceraldehyde into awake mice did not cause observable behavioral changes in the animals. At 15 s after i.v. injection, [U-^{13}C]glyceraldehyde could be seen in serum at 1.3 ± 0.2 mmol/L (n = 3), roughly corresponding to the 1:100 dilution of injecting 10 μL of [U-^{13}C]glyceraldehyde solution per gram bodyweight. This indicated rapid exit of glyceraldehyde from the circulation.

TABLE 1 Serum glucose and lactate and their percent ^{13}C enrichments.

	S-Glucose		S-Lactate	
	Mmol/L	% ^{13}C	Mmol/L	% ^{13}C
1 min	8.8 ± 2.8	2.9 ± 0.9	1.1 ± 0.7	8.6 ± 3.6
5 min	6.8 ± 1.3	2.2 ± 1.2	2.7 ± 1.3	5.7 ± 2.4
15 min	5.8 ± 1.4	2.6 ± 2.0	1.3 ± 0.4	5.8 ± 0.5
15 min + insulin	1.3 ± 0.4	0	1.7 ± 0.4	3.6 ± 1.4

Note: Fasted mice received [U-^{13}C]-D-glyceraldehyde, 1 μmol/g bodyweight, and were sacrificed at 1, 5, or 15 min. One group of mice was pretreated with insulin, 3 U/g bodyweight, to reduce s-glucose. Serum glucose and lactate were measured at sacrifice after injection of [U-^{13}C]-D-glyceraldehyde. Data are mmol/L or percent ^{13}C enrichment, mean ± SD values; n = 4 mice in each group.

I.v. administration of [U-^{13}C]glyceraldehyde led to detectable labeling of glucose and lactate in serum, but not of other metabolites, for example, glycerol, glycerate, or beta-hydroxybutyrate. Serum glucose, which was 5–9 mmol/L (Table 1), was ^{13}C-labeled in all carbon positions, and attained a ^{13}C-enrichment of 2%–3% in the C_1 position (which leads to the formation of lactate labeled in the C_3 position and to glutamate labeled in the C_4 position; Sonnewald, 2014) from 1 to 15 min after injection of [U-^{13}C]glyceraldehyde. Serum lactate, which was 1–3 mmol/L, was ^{13}C-labeled in all carbon positions, and attained a ^{13}C enrichment of 6%–8% in the C_3 position 1–15 min after injection of [U-^{13}C]glyceraldehyde.

To lower the serum concentration of ^{13}C-labeled glucose, mice were treated with insulin, which reduced blood glucose to 0.8 ± 0.2 mmol/L prior to injection of [U-^{13}C]glyceraldehyde. After injection, serum glucose was approximately 1 mmol/L (Table 1). At this stage, the animals were comatose, had lost the righting reflex,

and were non-responsive to tactile stimulation. I.v. injection of [U-^{13}C]glyceraldehyde into these animals did not cause detectable ^{13}C-labeling of serum glucose, but lactate was present in the serum of insulin-treated animals at approximately 1.7 mmol/L; its ^{13}C enrichment was ~3.6%, which was lower than in animals that did not receive insulin.

3.4 | ^{13}C labeling of metabolites in mouse brain from [U-^{13}C]glyceraldehyde

3.4.1 | Effect of insulin treatment

At 15–60 s after injection, traces of [U-^{13}C]glyceraldehyde could be seen in extracts of liver, lung, spleen, heart, and serum, but not brain. One minute after i.v. injection of [U-^{13}C]glyceraldehyde, only lactate was detectably ^{13}C-labeled in the brain. Lactate was labeled in all carbon positions; the percent enrichment of the C3 position is given in Figure 3. At 5–15 min, only lactate and glutamate were detectably ^{13}C-labeled in the brain. Glutamate was detectably labeled in the C_4 and C_5 positions only (indicating entry of uniformly ^{13}C-labeled acetyl-CoA into the tricarboxylic acid (TCA) cycle; Sonnewald, 2014). Figure 3 shows the percent enrichment of the C_4 position of glutamate (which corresponds to the C_3 position in lactate after entry of pyruvate into the TCA cycle via pyruvate dehydrogenase; Sonnewald, 2014).

At 5 min, the percent ^{13}C enrichment of lactate (~4%) was more than twice that of glutamate (~1.6%; Figure 3b). At 10 and 15 min after injection of [U-^{13}C]glyceraldehyde, the ^{13}C-labeling of glutamate had increased, reflecting the passage of ^{13}C-labeled substrate into the TCA cycle with time. ^{13}C-Labeling of glutamine and aspartate could not be seen, but ^{13}C-labeling of the C_2 position of GABA (which corresponds to the C_4 position of glutamate) could be seen faintly in two out of four animals.

The ^{13}C enrichment of brain lactate was higher than the enrichment of serum glucose at both 5 and 15 min ($p = 0.01$, $t = 5$, df = 3; paired, two-tailed t-test; compare Figure 3 and Table 1), indicating that cerebral metabolism of ^{13}C-labeled serum glucose could not explain the ^{13}C-labeling of brain lactate. The ^{13}C-enrichment of lactate was similar in serum and brain (compare Figure 3 and Table 1).

Insulin treatment led to a decrease in brain levels of alanine and glutamate (even after injection of [U-^{13}C]glyceraldehyde; Table 2), reflecting the reduced availability of pyruvate under hypoglycemia. Concomitantly, there was an increase in the level of aspartate, in agreement with previous studies (Engelsen & Fonnum, 1983; Gundersen et al., 2001; Tews et al., 1965), reflecting reduced availability of acetyl-CoA and accumulation of oxaloacetate, which equilibrates with aspartate.

As stated above, during insulin-induced hypoglycemia, ^{13}C-labeled glucose could not be detected in serum (Table 1). Under this condition, brain glutamate attained a percent ^{13}C enrichment that was higher than (at 10 min) or similar to (at 15 min) that was seen without insulin treatment (Figure 3), meaning that ^{13}C-labeling of brain glutamate from [U-^{13}C]glyceraldehyde did not depend on the formation of ^{13}C-labeled serum glucose. Further, under hypoglycemia, ^{13}C-labeled lactate could not be detected in the brain in agreement with a reduction in cerebral NADH levels under glucose deprivation (Bryan Jr. & Jöbsis, 1986; Garofalo et al., 1988), which would prevent the reduction of pyruvate into lactate.

3.5 | ^{13}C labeling of metabolites in mouse liver

Five minutes after i.v. injection of [U-^{13}C]glyceraldehyde, ^{13}C-labeled glucose and lactate could be detected in the liver. The ^{13}C enrichments of liver glucose and lactate were 5.2 ± 1.1% and 2.9 ± 0.3%, respectively. Fifteen minutes after injection of [U-^{13}C]glyceraldehyde,

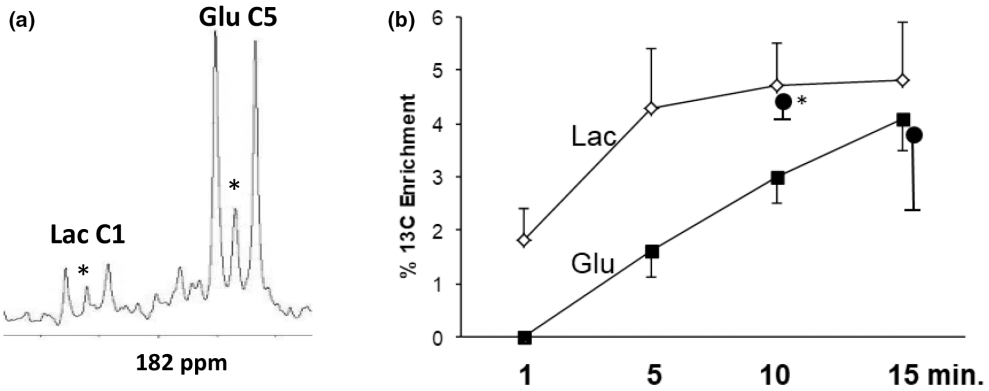

FIGURE 3 ^{13}C Enrichment of lactate and glutamate in brain after i.v. injection of [U-^{13}C]-D-glyceraldehyde into fasted mice. (a) Typical ^{13}C NMR spectrum showing ^{13}C-labeling of lactate C_1 and glutamate C_5 15 min after injection of [U-^{13}C]-D-glyceraldehyde. The middle single peaks (*) represent naturally abundant ^{13}C in lactate and glutamate; the larger peaks on each side of the single peak originate from [U-^{13}C]-D-glyceraldehyde. (b) Fasted mice received [U-^{13}C]-D-glyceraldehyde i.v. and were killed after 1–15 min. Two groups of mice were made hypoglycemic with insulin prior to injection of [U-^{13}C]-D-glyceraldehyde; in these mice, glutamate (filled circles) was ^{13}C-labeled, and lactate was not. Data are percent ^{13}C enrichment as determined from lactate C_3 and glutamate C_4, means ± SD values; $n = 4$ mice in each group. *: different from ^{13}C enrichment of glutamate in normoglycemic animals; $p = 0.014$, $t = 3.30$, df = 6. Glu, glutamate; Lac, lactate.

TABLE 2 Amino acid levels in brain and liver and lactate in brain.

Brain	Glu	Asp	Ala	GABA	Gln	Lac
5 min	9.3 ± 0.8	2.6 ± 0.4	0.5 ± 0.03	1.5 ± 0.06	2.4 0.08	100 ± 32%
15 min	9.1 ± 0.8	2.6 ± 0.03	0.4 ± 0.03	1.4 ± 0.2	2.0 ± 0.4	82 ± 22%
15 min + insulin	7.7 ± 0.3[a]	2.9 ± 0.08[b]	0.3 ± 0.02[c]	1.4 ± 0.1	2.6 ± 0.1	25 ± 30[d]
Liver	**Glu**	**Asp**	**Ala**	**GABA**	**Gln**	
5 min	3.1 ± 0.5	0.85 ± 0.18	2.6 ± 0.5	0	0.66 ± 0.17	n.d.
15 min	2.6 ± 0.4	0.50 ± 0.06	0.9 ± 0.2	0	0.8 ± 0.2	n.d.
15 min + insulin	2.4 ± 0.5	0.62 ± 0.08[e]	1.0 ± 0.2	0	0.4 ± 0.09[f]	n.d.

Note: Fasted mice received [U-^{13}C]-D-glyceraldehyde, 1 μmol/g bodyweight, and were sacrificed at 5 or 15 min. One group of mice was pretreated with insulin, 3 U/g bodyweight, to reduce serum glucose level, and was killed at 15 min after [U-^{13}C]-D-glyceraldehyde. Data for amino acids are nmol/mg tissue wet weight, data for lactate are percent of value at 5 min, as calculated from the ^{13}C NMR spectra; mean ± SD values; $n = 4$ mice in each group. Statistical comparison was done of groups that survived for 15 min and received or did not receive insulin (2-tailed Student's *t*-test). Superscripts: different from animals that did not receive insulin; a: $p = 0.016$, $t = 3.34$; b: $p = 0.0003$; $t = 7.29$; c: $p = 0.0011$, $t = 5$ and 0.83; d: $p = 0.022$, $t = 3.06$; e: $p = 0.046$, $t = 2.50$; f: $p = 0.0040$, $t = 4.53$; degrees of freedom was 6 for all tests. Lactate was detectable in the brains of only two out of four animals treated with insulin, and the mean and SD values include these as zero values.

Abbreviations: Ala, alanine; Asp, aspartate; GABA, γ-aminobutyric acid; Gln, glutamine; Glu, glutamate; Lac, lactate.

TABLE 3 Enzyme activities. Aldehyde dehydrogenase and reductase activities in homogenates of mouse brain or liver with D-glyceraldehyde as substrate.

	Brain (nmol/mg tissue/min)	Liver (nmol/mg tissue/min)
Aldehyde dehydrogenase	0.28 ± 0.04	2.6 ± 0.3
Aldehyde reductase	0.27 ± 0.07	1.1 ± 0.2
Glyoxalase I	13 ± 2	n.d.
Glyoxalase II	2.8 ± 0.6	n.d.

Note: Glyoxalase I and II were only measured in brain homogenates. Data are nmol/mg tissue wet weight × min^{-1}; mean ± SD values; $n = 5$ samples per group; 5 mice were used for aldehyde dehydrogenase and reductase measurements, another 5 mice were used for glyoxalase I and II measurements.

Abbreviation: n.d., not determined.

the ^{13}C enrichments of liver glucose and lactate were 5.5 ± 1.6% and 3.1 ± 0.9%, respectively, which was similar to the enrichments at 5 min.

In liver, insulin treatment (+ injection of [U-^{13}C]glyceraldehyde) caused the level of glutamine to drop by 50% and the level of aspartate to increase by 24% (Table 2). Liver extracts from hypoglycemic animals were not analyzed with ^{13}C NMRS.

3.6 | Activities of enzymes of glyceraldehyde dehydrogenase metabolism

The aldehyde dehydrogenase activity in mouse brain with [U-^{13}C]glyceraldehyde as substrate at saturating concentration (3 mmol/L) was ~0.28 nmol/mg tissue wet weight/min; in liver, it was approximately 10 times higher (Table 3). The D-glyceraldehyde-reducing activity in mouse brain, with [U-^{13}C]glyceraldehyde as substrate, was ~0.27 nmol/mg tissue/min, which is similar to previously reported values (Aragno et al., 2005; Cao Danh et al., 1984). The activity in liver was approximately 4 times higher, and at a level that was similar to a value reported by Hagopian et al. (2008). These aldehyde dehydrogenase and reductase activities were lower than the calculated glyceraldehyde diol dehydration rate (see "Rate of glyceraldehyde dehydration"), and so diol dehydration should not be rate limiting for the enzyme activities. The activities of glyoxalase I and II in brain were broadly similar to previously reported values in cultured neurons (Bélanger et al., 2011).

4 | DISCUSSION

4.1 | Metabolism constitutes a detoxification mechanism for glyceraldehyde in the brain

An initial finding in this study was that [U-^{13}C]glyceraldehyde could not be identified in the brain after i.v. injection although it could be seen in several other organs up to 1 min after i.v. injection. In the brain, only ^{13}C-labeled lactate, glutamate, and, in some animals, GABA could be identified. This finding indicated immediate uptake of extracellular glyceraldehyde by brain cells with subsequent metabolism through glycolysis and the TCA cycle.

Glyceraldehyde was overwhelmingly present in its hydrated diol form in aqueous solution; however, we show that the dehydration of the aldehyde group greatly exceeds cerebral glyceraldehyde metabolism, and so diol dehydration could not be rate-limiting. To the extent that glyceraldehyde is neurotoxic (Choei et al., 2004; Fawver et al., 2012; Ooi et al., 2022; Piccirillo et al., 2023), its metabolism may be considered a glyceraldehyde detoxification mechanism. This mechanism may be inhibited in Alzheimer's disease, in which cerebral glucose metabolism (and thereby possibly glyceraldehyde metabolism) is reduced even in the preclinical stage of the disease (Mosconi et al., 2008).

In the brain, [U-^{13}C]glyceraldehyde probably underwent metabolism in different directions (reduction, oxidation,

phosphorylation), leading to the formation of various ^{13}C-labeled intermediates. The level of each of these intermediates was likely too low to allow detection by ^{13}C NMRS before the ^{13}C-label accumulated in the larger lactate and glutamate pools, leading to ^{13}C NMRS detection.

Some energy substrates, such as acetate and propionate, will, when isotopically labeled, yield a higher percent enrichment of glutamine than of glutamate in the brain (Cerdan et al., 1990; Hassel et al., 1995; Van den Berg et al., 1969), indicating their predominant metabolism in glial cells, because glia, unlike neurons, express glutamine synthetase (Martinez-Hernandez et al., 1977; Tansey et al., 1991; Zhou et al., 2020). Isotopically labeled glycerol, in contrast, has been shown to label GABA more strongly than glutamate, suggesting its predominant metabolism in GABAergic neurons (Nguyen et al., 2003). The observation in the present study that glutamate was the only amino acids that was consistently ^{13}C-labeled suggests that the metabolism of [U-^{13}C]glyceraldehyde did not primarily occur in glia or GABAergic neurons, but more generally in brain cells, including glutamatergic neurons. The ^{13}C-labeling of glutamate from [U-^{13}C]glyceraldehyde in the brain agrees with previous radiolabeling experiments (Hassel et al., 2015).

The concentration of glyceraldehyde handled metabolically by brain cells after injection of [U-^{13}C]glyceraldehyde may be roughly estimated from the brain level of glutamate (~9 nmol/mg wet weight) and its ^{13}C enrichment at 15 min (~4%), meaning that ~0.36 nmol glutamate/mg wet weight originated from [U-^{13}C]glyceraldehyde. Assuming an 80% brain water content (Papadopoulos et al., 2004), this value would correspond to a whole-brain concentration of glyceraldehyde of 450 μmol/L after injection of [U-^{13}C]glyceraldehyde. This value, which is well in excess of normal serum glyceraldehyde concentrations in mice and humans (~10 and ~3 μmol/L, respectively; Martin-Morales et al., 2021), is probably a minimum value because the ^{13}C-label was distributed in various metabolite pools before reaching glutamate.

The observation that insulin pretreatment abolished formation of ^{13}C-labeled lactate in the brain strongly suggests that [U-^{13}C]glyceraldehyde did not primarily enter the glyoxalase pathway leading to the metabolically inert D-lactate (Phillips & Thornalley, 1993; see Section 1), but rather that it was metabolized through glycolysis. Glycolytic metabolism of [U-^{13}C]glyceraldehyde leads to the formation of pyruvate, which during hypoglycemia would be channeled into the TCA cycle rather than being converted into L-lactate.

4.2 | Glyceraldehyde enters the brain from the circulation

^{13}C-Labeling of lactate and glutamate in the brain strongly suggested passage of [U-^{13}C]glyceraldehyde across the blood–brain barrier. However, to some degree, the i.v.-injected [U-^{13}C]glyceraldehyde underwent metabolism in peripheral organs, for example, the liver, leading to ^{13}C-labeling of serum glucose and lactate. Because we did not detect [U-^{13}C]glyceraldehyde itself in the brain, one may ask whether the ^{13}C-label entered the brain as [U-^{13}C]glyceraldehyde or ^{13}C-labeled glucose or lactate. For ^{13}C-labeled serum glucose and lactate to be credible precursors of ^{13}C-labeled brain lactate and glutamate, their percent ^{13}C enrichment should be greater than that of the brain metabolites. In this study, the percent ^{13}C enrichment of serum glucose was generally lower than that of brain lactate and could therefore not explain the ^{13}C-labeling of the latter. Further, in hypoglycemic animals, serum glucose was not detectably ^{13}C-labeled, and still brain glutamate was ^{13}C-labeled at, or above, control level. Therefore, ^{13}C-labeling of brain metabolites from [U-^{13}C]glyceraldehyde did not depend on the formation of ^{13}C-labeled serum glucose. The ^{13}C enrichment of serum lactate was similar to that of brain lactate and greater than that of brain glutamate in the absence of insulin treatment. Indeed, ^{13}C-labeled serum lactate has been shown to label brain metabolites, but at concentrations and ^{13}C enrichments far greater than those achieved in the present study (Duarte et al., 2015; Hassel & Bråthe, 2000). Under normoglycemia and normal serum lactate concentration, the extraction of lactate into the brain has been estimated at 15% in humans (Knudsen et al., 1991). This estimate agrees with findings in the pig of a 90-fold increase in the flux of lactate and pyruvate from blood to brain once the blood–brain barrier has been opened (Miller et al., 2018). Thus, the contribution of serum lactate to the ^{13}C-labeling of brain metabolites could be approximately 11%–15%. In agreement with this conclusion was the finding in hypoglycemic animals that the ^{13}C enrichment of serum lactate was the same as that of brain glutamate, which is not a reasonable precursor–product relationship. Our findings therefore indicate glyceraldehyde movement across the blood–brain barrier. However, we cannot exclude the possibility that aldehyde dehydrogenases in the blood–brain barrier (for review, see Hipólito et al., 2007) to some extent converted [U-^{13}C]glyceraldehyde into glycerate before further metabolism occurred.

5 | CONCLUSIONS

We provide data showing that glyceraldehyde crosses the blood–brain barrier from the circulation into the brain. This conclusion implies that blood-borne glyceraldehyde could contribute to AGE and beta-amyloid plaque formation in the brain. Further, we show that glyceraldehyde is metabolized by brain cells. To the extent that glyceraldehyde is neurotoxic, its metabolism constitutes a detoxification mechanism. Lastly, spontaneous diol dehydration is not rate-limiting for glyceraldehyde metabolism in the brain.

AUTHOR CONTRIBUTIONS

Bjørnar Hassel: Conceptualization; investigation; writing – original draft; methodology; writing – review and editing; supervision; formal analysis; project administration. **Kristian Sørnes:** Conceptualization; investigation; methodology; formal analysis; writing – review and editing; software. **Ahmed Elsais:** Investigation; writing – review and editing; formal analysis; data curation. **Patricia Reyes Cordero:** Investigation; formal analysis; writing – review and editing; data

curation. **Anne Sofie Frøland:** Investigation; writing – review and editing; formal analysis; data curation. **Frode Rise:** Conceptualization; supervision; software; project administration; writing – review and editing; methodology; investigation.

FUNDING INFORMATION

This research did not receive any specific grant from funding agencies in the public, commercial, or not-for-profit sectors.

CONFLICT OF INTEREST STATEMENT

None.

PEER REVIEW

The peer review history for this article is available at https://www.webofscience.com/api/gateway/wos/peer-review/10.1111/jnc.16158.

DATA AVAILABILITY STATEMENT

The data that support the findings of this study are available from the corresponding author upon reasonable request.

REFERENCES

Angyal, S. J., & Wheen, R. G. (1980). The composition of reducing sugars in aqueous solution: Glyceraldehyde, erythrose, threose. *Australian Journal of Chemistry*, *33*, 1001–1011. https://doi.org/10.1071/CH9801001

Aragno, M., Mastrocola, R., Medana, C., Restivo, F., Catalano, M. G., Pons, N., Danni, O., & Boccuzzi, G. (2005). Up-regulation of advanced glycated products receptors in the brain of diabetic rats is prevented by antioxidant treatment. *Endocrinology*, *146*, 5561–5567. https://doi.org/10.1210/en.2005-0712

Arai, M., Nihonmatsu-Kikuchi, N., Itokawa, M., Rabbani, N., & Thornalley, P. J. (2014). Measurement of glyoxalase activities. *Biochemical Society Transactions*, *42*, 491–494. https://doi.org/10.1042/BST20140010

Bain, A. D., & Cramer, J. A. (1996). Slow chemical exchange in an eight-coordinated bicentered ruthenium complex studied by one-dimensional methods. Data fitting and error analysis. *Journal of Magnetic Resonance*, *118A*, 21–27. https://doi.org/10.1006/jmra.1996.0004

Bélanger, M., Yang, J., Petit, J. M., Laroche, T., Magistretti, P. J., & Allaman, I. (2011). Role of the glyoxalase system in astrocyte-mediated neuroprotection. *The Journal of Neuroscience*, *31*, 18338–18352. https://doi.org/10.1523/JNEUROSCI.1249-11.2011

Biessels, G. J., & Despa, F. (2018). Cognitive decline and dementia in diabetes mellitus: Mechanisms and clinical implications. *Nature Reviews. Endocrinology*, *14*, 591–604. https://doi.org/10.1038/s41574-018-0048-7

Bohren, K. M., Page, J. L., Shankar, R., Henry, S. P., & Gabbay, K. H. (1991). Expression of human aldose and aldehyde reductases. Site-directed mutagenesis of a critical lysine 262. *The Journal of Biological Chemistry*, *266*, 24031–24037. https://doi.org/10.1016/S0021-9258(18)54387-8

Bryan, R. M., Jr., & Jöbsis, F. F. (1986). Insufficient supply of reducing equivalents to the respiratory chain in cerebral cortex during severe insulin-induced hypoglycemia in cats. *Journal of Cerebral Blood Flow and Metabolism*, *6*(3), 286–291. https://doi.org/10.1038/jcbfm.1986.50

Cao Danh, H., Strolin Benedetti, M., & Dostert, P. (1984). Age-related changes in aldehyde reductase activity of rat brain, liver and heart. *Gerontology*, *30*, 159–166. https://doi.org/10.1159/000212624

Cerdan, S., Künnecke, B., & Seelig, J. (1990). Cerebral metabolism of [1,2-$^{13}C_2$]acetate as detected by in vivo and in vitro ^{13}C NMR. *The Journal of Biological Chemistry*, *265*(22), 12916–12926. https://doi.org/10.1016/S0021-9258(19)38247-X

Choei, H., Sasaki, N., Takeuchi, M., Yoshida, T., Ukai, W., Yamagishi, S., Kikuchi, S., & Saito, T. (2004). Glyceraldehyde-derived advanced glycation end products in Alzheimer's disease. *Acta Neuropathologica*, *108*, 189–193. https://doi.org/10.1007/s00401-004-0871-x

Dahlberg, D., Ivanovic, J., & Hassel, B. (2014). High extracellular concentration of excitatory amino acids glutamate and aspartate in human brain abscess. *Neurochemistry International*, *69*, 41–47. https://doi.org/10.1016/j.neuint.2014.03.001

Davies, J., Tomlinson, S., Elliott, A. C., & Best, L. (1994). A possible role for glyceraldehyde transport in the stimulation of HIT-T15 insulinoma cells. *The Biochemical Journal*, *304*, 295–299. https://doi.org/10.1042/bj3040295

Duarte, J. M., Girault, F. M., & Gruetter, R. (2015). Brain energy metabolism measured by ^{13}C magnetic resonance spectroscopy in vivo upon infusion of [3-^{13}C]lactate. *Journal of Neuroscience Research*, *93*(7), 1009–1018. https://doi.org/10.1002/jnr.23531

Engelsen, B., & Fonnum, F. (1983). Effects of hypoglycemia on the transmitter pool and the metabolic pool of glutamate in rat brain. *Neuroscience Letters*, *42*, 317–322. https://doi.org/10.1016/0304-3940(83)90281-1

European Union. (2010). *Directive 2010/63/EU of the European Parliament and of the Council of 22 September 2010 on the protection of animals used for scientific purposes*. http://data.europa.eu/eli/dir/2010/63/oj

Fawver, J. N., Schall, H. E., Petrofes Chapa, R. D., Zhu, X., & Murray, I. V. (2012). Amyloid-β metabolite sensing: Biochemical linking of glycation modification and misfolding. *Journal of Alzheimer's Disease*, *30*, 63–73. https://doi.org/10.3233/JAD-2012-112114

García-Jiménez, F., Zúñiga, O. C., García, Y. C., Cárdenas, J., & Cuevas, G. (2005). Experimental and theoretical study of the products from the spontaneous dimerization of DL- and D-glyceraldehyde. *Journal of the Brazilian Chemical Society*, *16*, 467–476. https://doi.org/10.1590/S0103-50532005000300022

Garofalo, O., Cox, D. W., & Bachelard, H. S. (1988). Brain levels of NADH and NAD^+ under hypoxic and hypoglycaemic conditions in vitro. *Journal of Neurochemistry*, *51*(1), 172–176. https://doi.org/10.1111/j.1471-4159.1988.tb04851.x

Gonzalez, S. V., Nguyen, N. H., Rise, F., & Hassel, B. (2005). Brain metabolism of exogenous pyruvate. *Journal of Neurochemistry*, *95*, 284–293. https://doi.org/10.1111/j.1471-4159.2005.03365.x

Guengerich, F. P., Sohl, C. D., & Chowdhury, G. (2011). Multi-step oxidations catalyzed by cytochrome P450 enzymes: Processive vs. distributive kinetics and the issue of carbonyl oxidation in chemical mechanisms. *Archives of Biochemistry and Biophysics*, *507*, 126–134. https://doi.org/10.1016/j.abb.2010.08.017

Gundersen, V., Fonnum, F., Ottersen, O. P., & Storm-Mathisen, J. (2001). Redistribution of neuroactive amino acids in hippocampus and striatum during hypoglycemia: A quantitative immunogold study. *Journal of Cerebral Blood Flow and Metabolism*, *21*, 41–51. https://doi.org/10.1097/00004647-200101000-00006

Hagopian, K., Ramsey, J. J., & Weindruch, R. (2008). Enzymes of glycerol and glyceraldehyde metabolism in mouse liver: Effects of caloric restriction and age on activities. *Bioscience Reports*, *28*, 107–115. https://doi.org/10.1042/BSR20080015

Hassel, B., & Bråthe, A. (2000). Cerebral metabolism of lactate in vivo: Evidence for neuronal pyruvate carboxylation. *Journal of Cerebral Blood Flow and Metabolism*, *20*, 327–336. https://doi.org/10.1097/00004647-200002000-00014

Hassel, B., Elsais, A., Frøland, A. S., Taubøll, E., Gjerstad, L., Quan, Y., Dingledine, R., & Rise, F. (2015). Uptake and metabolism of fructose by rat neocortical cells in vivo and by isolated nerve terminals in vitro. *Journal of Neurochemistry*, *133*, 572–581. https://doi.org/10.1111/jnc.13079

Hassel, B., Sonnewald, U., & Fonnum, F. (1995). Glial-neuronal interactions as studied by cerebral metabolism of [2-^{13}C]acetate and [1-^{13}C]glucose: An ex vivo ^{13}C NMR spectroscopic study. *Journal of Neurochemistry*, *64*(6), 2773–2782. https://doi.org/10.1046/j.1471-4159.1995.64062773.x

Hipólito, L., Sánchez, M. J., Polache, A., & Granero, L. (2007). Brain metabolism of ethanol and alcoholism: An update. *Current Drug Metabolism*, *8*, 716–727. https://doi.org/10.2174/138920007782109797

Hoffman, P. L., Wermuth, B., & von Wartburg, J. P. (1980). Human brain aldehyde reductases: Relationship to succinic semialdehyde reductase and aldose reductase. *Journal of Neurochemistry*, *35*, 354–366. https://doi.org/10.1111/j.1471-4159.1980.tb06272.x

Indiana University. (2022). *IACUC Policy for Dose Volumes in Laboratory Animals*. https://research.iu.edu/doc/compliance/animal-care/bloomington/iub-biacuc-dose-volumes-in-laboratory-animals.pdf

Jenkins, B. T., & Hajra, A. K. (1976). Glycerol kinase and dihydroxyacetone kinase in rat brain. *Journal of Neurochemistry*, *26*, 377–385. https://doi.org/10.1111/j.1471-4159.1976.tb04491.x

Kamp, C. W., Mursch, D. A., Stavinoha, W. B., & Medina, M. A. (1980). Measurement of mouse brain glucose utilization in vivo using [U-^{14}C]glucose. *Neurochemical Research*, *5*, 61–67. https://doi.org/10.1007/BF00964460

Keeler, J. (2010). *Understanding NMR spectroscopy, Ch. 9.6: Longitudinal dipolar relaxation of two spins* (2nd ed., pp. 267–274). John Wiley & Sons.

Knudsen, G. M., Paulson, O. B., & Hertz, M. M. (1991). Kinetic analysis of the human blood-brain barrier transport of lactate and its influence by hypercapnia. *Journal of Cerebral Blood Flow and Metabolism*, *11*(4), 581–586. https://doi.org/10.1038/jcbfm.1991.107

Leicht, W., Heinz, F., & Freimüller, B. (1978). Purification and characterization of aldehyde dehydrogenase from bovine liver. *European Journal of Biochemistry*, *83*, 189–196. https://doi.org/10.1111/j.1432-1033.1978.tb12083.x

Martinez-Hernandez, A., Bell, K. P., & Norenberg, M. D. (1977). Glutamine synthetase: Glial localization in brain. *Science*, *195*, 1356–1358. https://doi.org/10.1126/science.14400

Martin-Morales, A., Arakawa, T., Sato, M., Matsumura, Y., Mano-Usui, F., Ikeda, K., Inagaki, N., & Sato, K. (2021). Development of a method for quantitation of glyceraldehyde in various body compartments of rodents and humans. *Journal of Agricultural and Food Chemistry*, *69*, 13246–13254. https://doi.org/10.1021/acs.jafc.1c03177

Miller, J. J., Grist, J. T., Serres, S., Larkin, J. R., Lau, A. Z., Ray, K., Fisher, K. R., Hansen, E., Tougaard, R. S., Nielsen, P. M., Lindhardt, J., Laustsen, C., Gallagher, F. A., Tyler, D. J., & Sibson, N. (2018). ^{13}C pyruvate transport across the blood-brain barrier in preclinical hyperpolarised MRI. *Scientific Reports*, *8*(1), 15082. https://doi.org/10.1038/s41598-018-33363-5

Montagne, A., Nation, D. A., Sagare, A. P., Barisano, G., Sweeney, M. D., Chakhoyan, A., Pachicano, M., Joe, E., Nelson, A. R., D'Orazio, L. M., Buennagel, D. P., Harrington, M. G., Benzinger, T. L. S., Fagan, A. M., Ringman, J. M., Schneider, L. S., Morris, J. C., Reiman, E. M., Caselli, R. J., … Zlokovic, B. V. (2020). APOE4 leads to blood-brain barrier dysfunction predicting cognitive decline. *Nature*, *581*, 71–76. https://doi.org/10.1038/s41586-020-2247-3

Moon, K. H., Abdelmegeed, M. A., & Song, B. J. (2007). Inactivation of cytosolic aldehyde dehydrogenase via S-nitrosylation in ethanol-exposed rat liver. *FEBS Letters*, *581*, 3967–3972. https://doi.org/10.1016/j.febslet.2007.07.037

Mosconi, L., Pupi, A., & De Leon, M. J. (2008). Brain glucose hypometabolism and oxidative stress in preclinical Alzheimer's disease. *Annals of the New York Academy of Sciences*, *1147*, 180–195. https://doi.org/10.1196/annals.1427.007

Nguyen, N. H., Bråthe, A., & Hassel, B. (2003). Neuronal uptake and metabolism of glycerol and the neuronal expression of mitochondrial glycerol-3-phosphate dehydrogenase. *Journal of Neurochemistry*, *85*(4), 831–842. https://doi.org/10.1046/j.1471-4159.2003.01762.x

O'Brien, M. M., & Schofield, P. J. (1980). Polyol-pathway enzymes of human brain. Partial purification and properties of aldose reductase and hexonate dehydrogenase. *The Biochemical Journal*, *187*, 21–30. https://doi.org/10.1042/bj1870021

Ooi, H., Nasu, R., Furukawa, A., Takeuchi, M., & Koriyama, Y. (2022). Pyridoxamine and aminoguanidine attenuate the abnormal aggregation of β-tubulin and suppression of neurite outgrowth by glyceraldehyde-derived toxic advanced glycation end-products. *Frontiers in Pharmacology*, *13*, 921611. https://doi.org/10.3389/fphar.2022.921611

Papadopoulos, M. C., Manley, G. T., Krishna, S., & Verkman, A. S. (2004). Aquaporin-4 facilitates reabsorption of excess fluid in vasogenic brain edema. *The FASEB Journal*, *18*, 1291–1293. https://doi.org/10.1096/fj.04-1723fje

Phillips, S. A., & Thornalley, P. J. (1993). The formation of methylglyoxal from triose phosphates. Investigation using a specific assay for methylglyoxal. *European Journal of Biochemistry*, *212*, 101–105. https://doi.org/10.1111/j.1432-1033.1993.tb17638.x

Piccirillo, S., Preziuso, A., Cerqueni, G., Serfilippi, T., Terenzi, V., Vinciguerra, A., Amoroso, S., Lariccia, V., & Magi, S. (2023). A strategic tool to improve the study of molecular determinants of Alzheimer's disease: The role of glyceraldehyde. *Biochemical Pharmacology*, *218*, 115869. https://doi.org/10.1016/j.bcp.2023.115869

Rendina, A. R., Hermes, J. D., & Cleland, W. W. (1984). A novel method for determining rate constants for dehydration of aldehyde hydrates. *Biochemistry*, *23*, 5148–5156. https://doi.org/10.1021/bi00317a011

Serianni, A. S., Clark, E. L., & Barker, R. (1979). Carbon-13-enriched carbohydrates. Preparation of erythrose, threose, glyceraldehyde, and glycolaldehyde with ^{13}C-enrichment in various carbon atoms. *Carbohydrate Research*, *72*, 79–91. https://doi.org/10.1016/S0008-6215(00)83925-7

Sonnewald, U. (2014). Glutamate synthesis has to be matched by its degradation—where do all the carbons go? *Journal of Neurochemistry*, *131*(4), 399–406. https://doi.org/10.1111/jnc.12812

Stewart, M. A., Sherman, W. R., Kurien, M. M., Moonsammy, G. I., & Wisgerhof, M. (1967). Polyol accumulations in nervous tissue of rats with experimental diabetes and galactosaemia. *Journal of Neurochemistry*, *14*, 1057–1066. https://doi.org/10.1111/j.1471-4159.1967.tb09516.x

Tansey, F. A., Farooq, M., & Cammer, W. (1991). Glutamine synthetase in oligodendrocytes and astrocytes: New biochemical and immunocytochemical evidence. *Journal of Neurochemistry*, *56*, 266–272. https://doi.org/10.1111/j.1471-4159.1991.tb02591.x

Tews, J. K., Carter, S. H., & Stone, W. E. (1965). Chemical changes in the brain during insulin hypoglycaemia and recovery. *Journal of Neurochemistry*, *12*, 679–693. https://doi.org/10.1111/j.1471-4159.1965.tb06782.x

The Human Metabolome Database *The Human Metabolome Database*, *Version 4.0*. http://www.hmdb.ca/metabolites/HMDB0001051

University of British Columbia. (2021). *Standard operating procedures. TECH 03a Intravenous Tail Vein Injections in the Adult Mouse (2021)*. https://animalcare.ubc.ca/animal-care-committee/sops-policies-and-guidelines/standard-operating-procedures

Van den Berg, C. J., Krzalić, L., Mela, P., & Waelsch, H. (1969). Compartmentation of glutamate metabolism in brain. Evidence for the existence of two different tricarboxylic acid cycles in brain. *The Biochemical Journal*, *113*(2), 281–290. https://doi.org/10.1042/bj1130281

Xin, L., Lanz, B., Lei, H., & Gruetter, R. (2015). Assessment of metabolic fluxes in the mouse brain in vivo using ^{1}H-[^{13}C] NMR spectroscopy at 14.1 tesla. *Journal of Cerebral Blood Flow and Metabolism*, *35*, 759–765. https://doi.org/10.1038/jcbfm.2014.251

Zhang, Y., Xu, Z., Zhao, Y., & Zhang, X. (2019). Ab initio molecular dynamics simulation study of dissociation electron attachment to lactic

acid and isomer. *Scientific Reports*, *9*(1), 19532. https://doi.org/10.1038/s41598-019-56019-4

Zhou, Y., Eid, T., Hassel, B., & Danbolt, N. C. (2020). Novel aspects of glutamine synthetase in ammonia homeostasis. *Neurochemistry International*, *140*, 104809. https://doi.org/10.1016/j.neuint.2020.104809

SUPPORTING INFORMATION

Additional supporting information can be found online in the Supporting Information section at the end of this article.

How to cite this article: Hassel, B., Sørnes, K., Elsais, A., Cordero, P. R., Frøland, A. S., & Rise, F. (2024). Glyceraldehyde metabolism in mouse brain and the entry of blood-borne glyceraldehyde into the brain. *Journal of Neurochemistry*, *168*, 2868–2879. https://doi.org/10.1111/jnc.16158